Diffraction of x rays at a Bragg angle of $\pi/2$ (back reflection) with consideration of multiwave effects

V. G. Kohn,*) I. V. Kohn, and É. A. Manykin

Russian Research Center ''Kurchatov Institute'', 123182 Moscow, Russia
(Submitted 26 January 1999)
Zh. Éksp. Teor. Fiz. **116**, 940–952 (September 1999)

The energy dependence of the back reflectivity in the dynamical diffraction of x rays at a Bragg angle of $\pi/2$ (back diffraction) in perfect crystals of cubic symmetry (silicon) is investigated theoretically. In this case strict backscattering is realized only under the conditions of multiple diffraction. The features of the influence of multiple diffraction on back reflection in the energy range near the nuclear resonance radiation energy of 14.41 keV for ^{57}Fe nuclei, specifically in the six-wave case, including the silicon (1,9,9) reflection (with an energy of 14.57 keV), which can be investigated experimentally with high energy resolution (1 meV) using synchrotron radiation and a monochromator developed for nuclear resonant absorption, are thoroughly studied. It is shown that the back reflectivity observed under the conditions of multiple diffraction has several maxima on the plot of its energy dependence with a value at each maximum smaller than half, in contrast to two-wave diffraction, where there is one maximum with a value close to unity. © *1999 American Institute of Physics.* [S1063-7761(99)01309-8]

1. INTRODUCTION

The back reflection of x rays during diffraction on perfect crystals with a Bragg angle of $\pi/2$ (back diffraction) is known to occur only in a very narrow energy range with a relative width less than 10^{-6}, but has a relatively weak sensitivity to the angular divergence of the beam (no more than 10^{-3} rad). Since the construction of the dispersion surface introduced into the theory by Ewald[1] is impossible in the case under consideration, it initially appeared that a generalized solution of Maxwell's equations without linearization of the dispersion correction to the wave vector must be used to analyze back reflection.[2,3] In reality, the theory remains linearized to a high accuracy, and in terms of the deviation parameter from the Bragg condition it does not differ in any way from diffraction at a Bragg angle smaller than $\pi/2$ (Ref. 4).

A slight angular deviation of the beam for the direction corresponding to strict backscattering was used in the experimental investigations of back reflection in Refs. 5–7, since otherwise it was impossible to pass the incident beam through the opaque detector. This simultaneously permitted elimination of the multiwave effects and allowed the use of the theory of two-wave diffraction to describe the measured plots of the energy (temperature) and angular dependences of the reflectivity. Additional back reflection was employed to monochromatize the beam, and the convolution of two theoretical reflection curves was calculated simultaneously for comparison with experiment. Good agreement between the experimental temperature curve and the theoretical calculation was obtained in Ref. 7.

Nevertheless, strict backscattering (back diffraction) is of considerable interest in connection with the possibility of using it to create an x-ray analog of the familiar Fabry–Pérot interferometer (see, for example, Ref. 8 and the references therein). In this case very high monochromatization of the radiation is needed to ensure a long longitudinal (temporal) coherence length. The necessary degree of monochromatization is achieved with a safety margin using a ''Mössbauer monochromator,'' i.e., the nuclear resonant scattering of pulses of synchrotron radiation in conjunction with a time-window technique, under which a detector with a high temporal resolution, of the order of a nanosecond, permits isolation of only the scattered radiation delayed by nuclei. The latter has an energy width of the order of the width of the excited state of the nuclei Γ. Only the ^{57}Fe nuclear transition with an energy $E=14.413\,\text{keV}$ and a width $\Gamma=4.66\times10^{-6}\,\text{meV}$ has been used hitherto fairly widely. A transparent detector and a large crystal–detector distance must also be employed to measure strict backscattering. The incident (primary) synchrotron radiation pulse is also cut off using a time window.

Just such a measurement technique was recently first proposed and successfully implemented in Ref. 9. Sapphire (Al_2O_3) crystals, which did not have a sufficiently perfect crystal lattice, were used to eliminate the multiwave effects in Ref. 9. For this reason, despite the high angular collimation and the very high monochromaticity of the incident beam, the experimental curves differed from the results of a calculation based on the dynamical theory for perfect crystals.

Hitherto, only silicon crystals had a sufficiently perfect structure. In this case several reflections have energies close to $E=14.413\,\text{keV}$. They are the (3,5,11) reflection with $E=14.210\,\text{keV}$, the (0,4,12) reflection with $E=14.437\,\text{keV}$, and the (1,9,9) reflection with $E=14.572\,\text{keV}$. In all cases back reflection is realized under the conditions of multiple diffraction. The reflections indicated were recently measured in Ref. 10 at room tempera-

ture. An x-ray monochromator with a resolution of the order of 1 meV was used this time. Monochromators of such a type were widely used in the last few years in the Mössbauer facilities of third-generation synchrotron radiation sources (ESRF in France, APS in the U.S.A., and SPring-8 in Japan), in inelastic nuclear resonant absorption experiments (for the latest results on this subject, see Refs. 11 and 12 and the references therein) and were developed specifically for $E = 14.4\,\text{keV}$ with the possibility of scanning the energy in a small range.

Moreover, the use of back reflectivity peaks in silicon as reference marks on the energy scale of such a monochromator permits measurement of the energy of the nuclear transition itself to a higher accuracy in comparison to other methods. Just such a problem was solved in Ref. 10. For this purpose, in particular, it is necessary to know how the multiwave effects influence the form of the back reflectivity peak. Thus, an investigation of strict backscattering with consideration of the multiwave effects has practical value in addition to being of purely physical interest. The (3,5,11) and (0,4,12) reflections correspond to 24-wave diffraction. They will be studied at a later date. The present work is devoted to an analysis of back reflection with consideration of multiwave effects in the case of the silicon (1,9,9) reflection, which corresponds to 6-wave diffraction. The dynamical theory of the diffraction of plane waves in matrix form and the scheme for the computer calculations are presented in the next section. The scattering geometry and the results of the numerical calculations are presented in Sec. 3. Section 4 offers a qualitative analysis of the influence of multiwave corrections on two-wave diffraction in ranges of parameters where they can be regarded as a perturbation. It provides partial explanations for the numerical results obtained.

2. MATRIX FORM OF THE DYNAMICAL THEORY OF THE MULTIPLE DIFFRACTION OF PLANE WAVES

The theory is devised for a monochromatic plane wave with a frequency ω and a wave vector $\mathbf{K}_0$. Real radiation can always be represented as a superposition of plane waves, and we assume that the different frequencies and directions of the wave vectors are incoherent. Thus, the intensity of the back-reflected radiation for a monochromatic plane wave must be calculated, and then the result must be averaged over the finite angular and frequency (energy) ranges corresponding to the results of the specific experiment. When the conditions for multiple diffraction in a crystal in the form of a plane-parallel plate with an internal normal $\mathbf{n}$ to the entrance surface of the crystal are satisfied, an incident wave with the electric field intensity

$$\mathbf{E}_0(\mathbf{r},t)=\mathbf{E}_0\exp(i\mathbf{K}_0\cdot\mathbf{r}-i\omega t) \tag{1}$$

corresponds to the superposition of truncated Bloch waves:

$$\mathbf{E}(\mathbf{r},t)=\sum_j \lambda_j \sum_m \mathbf{E}_{mj}\exp(i\mathbf{k}_{mj}\cdot\mathbf{r}-i\omega t),$$

$$\mathbf{k}_{mj}=\mathbf{K}_0+\mathbf{h}_m+\varepsilon_j\mathbf{n}, \tag{2}$$

which contains only reciprocal-lattice vectors $\mathbf{h}_m$ of the crystal that satisfy the Bragg condition $(\mathbf{K}_0+\mathbf{h}_m)^2\approx\mathbf{K}_0^2$ to an assigned accuracy of the order of the amplitude χ_m of the diffraction scattering from one wave to another. The subscript j labels the possible solution, and λ_j is the degree of excitation of the respective solution in the crystal for an assigned incident wave. It is found from the boundary conditions.

When solutions in the form (2) are plugged into Maxwell's equation for the amplitude of the electric field, the following approximations are made to an accuracy of the order of $\chi_0\approx10^{-6}$.

1) The electric field is assumed to be transverse:

$$\mathbf{E}_{mj}=\sum_s E_{msj}\mathbf{e}_{ms}, \tag{3}$$

where $s=\pi,\sigma$ is the polarization index, and the unit vectors $\mathbf{e}_{ms}$ specify the polarization direction in beam m in a plane perpendicular to the unit vector $\mathbf{s}_m$, which is parallel to $\mathbf{K}_0+\mathbf{h}_m$.

2) Only the first power of the dispersion correction ε is taken into account in the equations. This corresponds to the approximation of generalized geometric optics in the small-angle case.

3) Averaging of the equation over a unit cell of the crystal is performed for the purpose of eliminating the fast variables with a variation length of the order of the wavelength of x rays from the calculations.

4) Only the dipolar interaction of the electromagnetic wave with the medium is taken into account (the accuracy of this approximation is poorer than that of the preceding approximations, but in all cases, except the anomalous transmission effect, it is sufficient).

The approximations indicated allow us to write equations separately for each of the scalar amplitudes E_{msj} in the following form (for further details, see Refs. 1 and 13):

$$\left(\frac{\gamma_m}{K}\varepsilon+\alpha_m\right)E_{ms}=\sum_{m',s'} g_{mm'}^{ss'}E_{m's'}, \tag{4}$$

where $K=\omega/c$ is the wave number, c is the speed of light,

$$\gamma_m=(\mathbf{s}_m\cdot\mathbf{n}),\quad g_{mm'}^{ss'}=\chi_{m-m'}(\mathbf{e}_{ms}\cdot\mathbf{e}_{m's'}),$$

$$\alpha_m=[(\mathbf{K}_0+\mathbf{h}_m)^2-\mathbf{K}_0^2]/K^2, \tag{5}$$

and $\chi_{m-m'}$ is the Fourier component of the polarizability of the crystal in the reciprocal-lattice vector $\mathbf{h}_m-\mathbf{h}_{m'}$.

To describe the calculation scheme in matrix form it is convenient to combine the two indices m and s into one, for which we retain the notation m. The index m thus runs through the values $0\pi,0\sigma,1\pi,1\sigma,\ldots,(n-1)\pi,(n-1)\sigma$ in the n-wave case. Going over to the new amplitudes, $B_{mj}=\gamma_m^{1/2}E_{mj}$, we can rewrite the system of equations (4) in the form characteristic of many dynamical systems (electrons, phonons, etc.), i.e., as the eigenvalue problem

$$\varepsilon B_m=\sum_{m'} G_{mm'}B_{m'} \tag{6}$$

for the kinematic scattering matrix

$$G_{mm'}=H_{mm'}-A_m\delta_{mm'}=K(\gamma_m\gamma_{m'})^{-1/2}\times(g_{mm'}-\alpha_m\delta_{mm'}), \quad (7)$$

where $\delta_{mm'}$ is a Kronecker delta, which is equal to zero when $m\neq m'$ and to unity when $m=m'$.

The matrix $G_{mm'}$ has a rank of $2n$. Accordingly, there are $2n$ different characteristic solutions of the problem (6), which are distinguished by the index j. Unlike other dynamical systems, the matrix $G_{mm'}$ is non-Hermitian, since the matrix $g_{mm'}$ is non-Hermitian in the general case with consideration of the absorption of x rays. However, the parts of $g_{mm'}$ which describe scattering and absorption separately are Hermitian. Nevertheless, the matrix $G_{mm'}$ is still non-Hermitian even for a nonabsorbing crystal, if among the parameters γ_m there are some which have negative values. This always occurs in the case of back diffraction. Therefore, the eigenvalues ε of the problem, i.e., the dispersion corrections to the wave vectors, are complex even for a nonabsorbing crystal. In addition, some of them have a negative imaginary part, which corresponds to growth of the Bloch waves as they move into the crystal. This, in turn, causes some difficulty in solving the boundary-value problem by numerical methods on a computer.

The general solution of the boundary-value problem in a form which is stable toward increasing Bloch waves was given in Refs. 14 and 15. Below we shall briefly formulate the solution method used. For this purpose, we order the elements in the matrix of eigenvectors B_{mj} so that the index m corresponds to decreasing values of the parameter γ_m and the index j corresponds to decreasing values of the imaginary part of the eigenvalue ε_j''. If the number of Laue beams corresponding to the passage of radiation through the crystal plate for which $\gamma_m>0$ is equal to n_L, then the number of values of m corresponding to these waves and the number of solutions with a positive imaginary part of the eigenvalue ($\varepsilon_j''>0$) are equal to the same number $2n_L$. We denote the set of such values of the indices m and j by the single index L, and we denote the set of remaining values by the single index B. This allows us to divide the complete matrix of eigenvectors B_{mj} obtained as a result of the numerical solution of (6) into the four submatrices B_{LL}, B_{LB}, B_{BL}, and B_{BB}, of which the diagonal matrices B_{LL} and B_{BB} are strictly square, and the off-diagonal matrices are rectangular in the general case. The set of amplitudes for the reflection of Laue-type plane waves ($\gamma_m>0$) into Bragg-type plane waves ($\gamma_m<0$) is described by the block M_{BL} of the complete dynamical scattering matrix.

In this paper we analyze the back reflectivity in the approximation of a thick absorbing crystal, in which the increasing Bloch waves can be completely neglected. In this case the block of the dynamical scattering matrix of interest to us is described by the simple expression

$$M_{BL}=B_{BL}(B_{LL})^{-1}. \quad (8)$$

If the incident plane wave has the index 0 and is polarized in the s state (these conditions correspond to synchrotron radiation) and if the back-reflected wave has the index $k=n-1$ and its polarization state is not analyzed, then the experimentally measured reflectivity is described by the expression

$$R_{k0}^{(s)}=\sum_{s'}|M_{ks',0s}|^2. \quad (9)$$

The parameters of the problem are the components of the vector $\mathbf{q}=\mathbf{K}_0+\mathbf{h}_k/2$, which describe small deviations of the wave vector of the incident wave from the direction corresponding to strict backscattering $\mathbf{K}_0^{(0)}=-\mathbf{h}_k/2$. It is convenient to represent the vector $\mathbf{q}$ in the form

$$\mathbf{q}=K(\theta_1\mathbf{e}_{0\pi}+\theta_2\mathbf{e}_{0\sigma}+\theta_\omega\mathbf{s}_0), \quad (10)$$

where the parameters θ_1 and θ_2 describe the angular deviations of the incident beam and $\theta_\omega=(\omega-\omega_c)/\omega_c$ describes the spectral back reflection line sought. The critical frequency is $\omega_c=c|\mathbf{h}_k|/2$, the critical wavelength is $\lambda_c=2d_k$, where d_k is the interplanar distance for the back-reflecting atomic planes, and the crystal photon energy (in keV) is $E_c=12.4/\lambda_c$, where λ_c is measured in angstroms. With consideration of (10), the parameters of the deviation from the Bragg condition in the linear approximation with respect to $\mathbf{q}$ equal

$$\alpha_m=2(\mathbf{h}_m\cdot\mathbf{q})/K^2=2K^{-1}[(\mathbf{h}_m\cdot\mathbf{e}_{0\pi})\theta_1+(\mathbf{h}_m\cdot\mathbf{e}_{0\sigma})\theta_2+(\mathbf{h}_m\cdot\mathbf{s}_0)\theta_\omega]. \quad (11)$$

In experiments the incident beam always has a finite angular divergence, and the monochromator has a finite width. For simplicity, we assume that the shape of the angular and frequency spectra of the monochromator is rectangular. Thus, the spectral reflection line interesting us can be calculated from the formula

$$\overline{R_{k0}^{(s)}}(\theta_\omega)=\frac{1}{T_\theta^2T_\omega}\int d\theta_{\omega'}\int d\theta_1 d\theta_2 R_{k0}^{(s)}(\theta_1,\theta_2,\theta_{\omega'}-\theta_\omega), \quad (12)$$

where T_θ and T_ω specify the angular and frequency widths of the monochromator, respectively, and the integration is performed in these limits.

3. (1,9,9) BACK REFLECTION IN SILICON UNDER THE CONDITIONS OF SIX-WAVE DIFFRACTION. GEOMETRY AND CALCULATION RESULTS

In crystals of cubic symmetry strict backscattering on a reciprocal-lattice vector with fairly large Miller indices is always accompanied by reflection into other reciprocal-lattice vectors, which satisfy the Bragg conditions as a consequence of the symmetry of the crystal lattice. For example, in a silicon crystal the (1,9,9) reflection occurs simultaneously with the (−4,0,4), (−4,4,0), (5,9,5), and (5,5,9) reflections, so that six-wave diffraction is realized when the Bragg conditions are strictly satisfied. In this case the truncated Bloch waves are sums of plane waves with the wave vectors $\mathbf{k}_m=\mathbf{K}_0+\mathbf{h}_m$, which have the following values in units of π/a, where a is the lattice constant, in the coordinate system of the reciprocal lattice of the crystal:

(−0.5,−4.5,−4.5); (−4.5,−4.5,−0.5);

(−4.5,−0.5,−4.5);

(4.5,4.5,0.5); (4.5,0.5,4.5); (0.5,4.5,4.5).

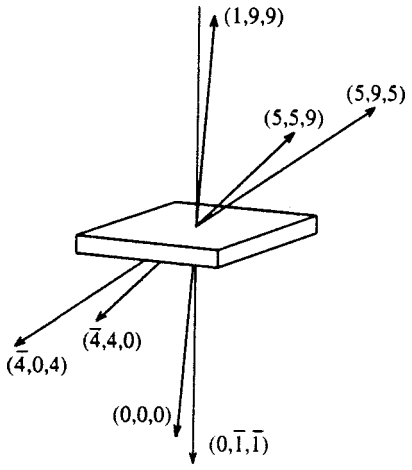

FIG. 1. Directions of the diffracted beams relative to the crystal plane. The plane of the plate is perpendicular to the $(0,-1,-1)$ direction.

Let the crystal plate be cut so that the normal to the surface is parallel to the $(0,-1,-1)$ direction. In this case the parameters γ_m are equal to 0.997, 0.554, 0.554, -0.554, -0.554, and -0.997, respectively, i.e., we have three Laue-type waves and three Bragg-type waves. Figure 1 shows the directions of the diffracted beams relative to the crystal plate. The polarization vectors in each wave can be chosen arbitrarily. Taking into account the scattering symmetry, we choose the polarization vectors in the following manner. The vector $\mathbf{e}_{0\pi}$ is parallel to the $(0,1,-1)$ direction, and the remaining vectors are defined according to the formulas

$$\mathbf{e}_{m\sigma}=\mathbf{s}_m\times\mathbf{e}_{0\pi},\quad \mathbf{e}_{m\pi}=\mathbf{e}_{m\sigma}\times\mathbf{s}_m. \tag{13}$$

At the same time, the set of three vectors $\mathbf{e}_{0\pi}$, $\mathbf{e}_{0\sigma}$, and $\mathbf{s}_0$ is used to resolve the vector $\mathbf{q}$, as follows from formula (10).

The numerical values for the Fourier components χ_m of the polarizability of the crystal were obtained using Stepanov's X0H program. When this work was carried out, this program was freely available on the Internet.[16]

As we know, a symmetric 2×2 matrix with diagonal elements equal to one another has eigenvectors with components that are equal in absolute value and thus corresponds exactly to dynamical diffraction. Therefore, the centers of the two-wave reflection maxima are determined with consideration of the dynamical displacement of the parameters by the relations $A_m=H_{mm}-H_{00}$, which depend, among other things, on the parameters γ_m, rather than by the conditions $\alpha_m=0$. In the case under consideration these conditions have the following form in microradians (μrad):

$$\begin{aligned}
&(-4,0,4):\ -0.118\theta_1-0.176\theta_2-0.105\,\theta_\omega=-0.271\\
&(-4,4,0):\ +0.118\theta_1-0.176\theta_2-0.105\,\theta_\omega=-0.271\\
&(5,9,5):\ -0.118\theta_1-0.176\theta_2+0.429\,\theta_\omega=+0.949\\
&(5,5,9):\ +0.118\theta_1-0.176\theta_2+0.429\,\theta_\omega=+0.949\\
&(1,9,9):\ +0.296\,\theta_\omega=+0.678.
\end{aligned} \tag{14}$$

As follows from these conditions, two-wave back reflection does not depend on the angular variables, but the reflection maximum is shifted with respect to the photon energy by $\Delta E=\Delta_0=E_c\theta_\omega^{(0)}=33.4$ meV.

It is difficult to graphically represent the three-dimensional dependence of the reflectivity $R_{k0}^{(s)}(\Delta E,\theta_1,\theta_2)$, where $\Delta E=E_c\theta_\omega$. Therefore, we shall present and discuss only fragments of the general dependence. Figure 2 shows the dependence of the back reflectivity for the (1,9,9) reflection in the $(\Delta E,\theta_2)$ plane of arguments at $\theta_1=0$, and Fig. 3 presents the dependence in the $(\Delta E,\theta_1)$ plane at $\theta_2=0$ for both polarization states in the incident wave. As follows from the calculations represented in these figures, the two-wave band of the back reflection maximum due to (1,9,9) diffraction vanishes as the multiwave region of parameters is approached. In addition, it is easy to discern the presence of additional reflection bands in regions where the Bragg condition for (1,9,9) diffraction is not satisfied but the Bragg condition for other reflections is satisfied.

While the value of the reflectivity increases as we move along the two-wave band of the (1,9,9) reflection from the center to the edges, it decreases as we move along the additional bands. This is because the additional reflection bands have an essentially multiwave character. The slope of these bands relative to the energy axis in the $(\Delta E,\theta_2)$ plane at $\theta_1=0$ is determined from the conditions (14). For example, the conditions for two-wave diffraction in the (5,9,5) and (5,5,9) reflections are satisfied in the line at $\theta_2=0.167\Delta E-5.932$. Here and below, the shift of the photon energy ΔE is measured in millielectron volts (meV). This means that three-wave (0,0,0; 5,9,5; 5,5,9) diffraction occurs in this line. The (1,9,9) back reflection is weak (kinematic), but it is enhanced because of the simultaneous presence of several strong waves. A more detailed analysis is given in the following section.

As follows for Fig. 2, there is a second line of additional reflection. It corresponds to three-wave $(-4,0,4;-4,4,0;1,9,9)$ diffraction. The Bragg condition for this case is obtained by subtracting the condition for the $(-4,0,4)$ reflection from the condition for the (1,9,9) reflection in formulas (14). At $\theta_1=0$ a simple calculation then permits determination of the equation of the second line at $\theta_2=-0.156\Delta E+5.932$. The two lines cross at the point $\Delta E=36.73$ meV, $\theta_2=0.742$ μrad. The lines split at the crossing point, and there is symmetry of the (1,9,9) back reflectivity in the split lines relative to the change in the sign of the quantity $\theta_2-0.742$, although the physical conditions for reflection on both sides of the symmetric pattern are different. In one case the (1,9,9) reflection is a disturbance in the Bloch wave, where the strong waves are the (0,0,0), (5,9,5), and (5,5,9) waves. In the other case the (1,9,9) wave is a strong wave together with the $(-4,0,4)$ and $(-4,4,0)$ waves, but the perturbation is a component in the incident (0,0,0) band; therefore this Bloch wave is weakly excited in the crystal. The presence of polarization in the incident wave weakly influences the two-wave band of the (1,9,9) reflection, but has a very significant effect on the additional reflection bands.

The dependence shown in Fig. 3 is even more compli-

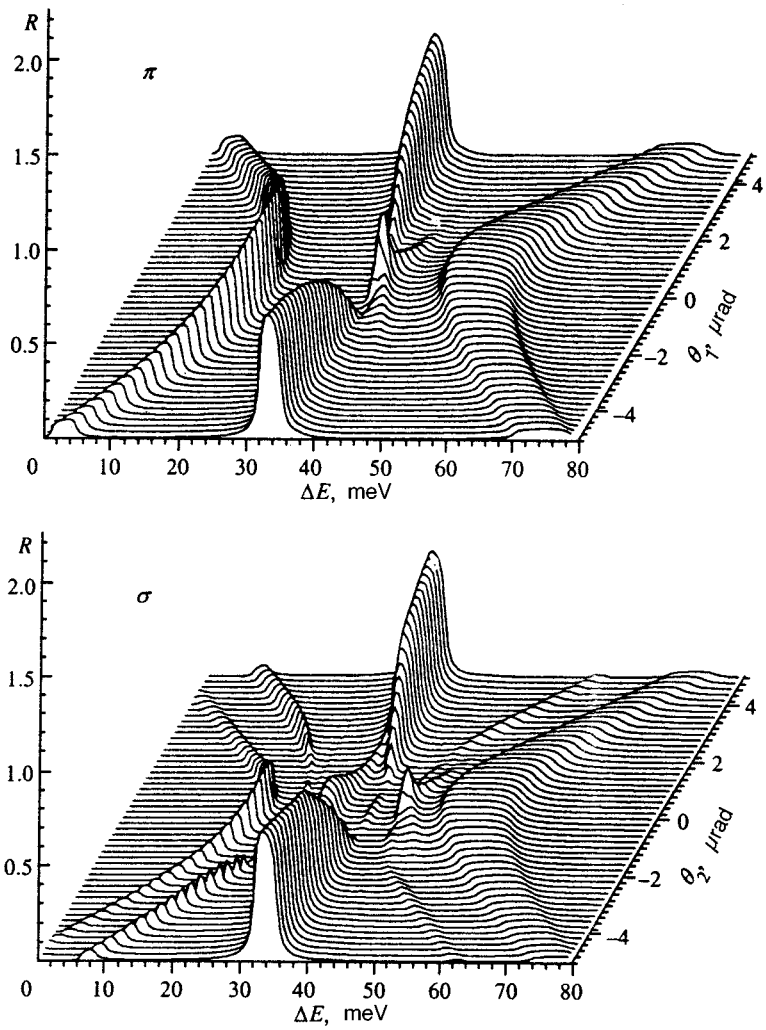

FIG. 2. Dependence of the reflectivity for (1,9,9) back reflection at $\theta_1=0$ for two polarization states of the incident wave (π and σ).

cated. The two-wave diffraction in the (0,0,0; 5,9,5) and (0,0,0; 5,5,9) reflections now takes place in the lines at $\theta_2=\pm 0.249$ ($\Delta E-32.2$). The additional reflection bands are strongly split for both polarization states. In addition, two-wave ($-4,4,0;1,9,9$) and ($-4,0,4;1,9,9$) bands are displayed in the lines at $\theta_2=\pm 0.239$ ($\Delta E-33.7$). The bands are closely spaced, although they do not coincide with one another. Therefore, the two-wave case with strong renormalization of the scattering parameters is partially realized here.

The experimental observation of the dependences of the reflectivity presented in this paper requires a strongly collimated (less than 1 μrad^2) and monochromatized (of the order of 1 meV) beam. If the beam has finite collimation and is not scanned over the angle, the dependence of the back reflectivity on the photon energy shift ΔE can be obtained by integrating over the angular variables θ_1 and θ_2 in assigned limits [see formula (12)]. Figure 4 shows the back reflection energy spectra for $T_\omega=0$ and $T_\theta=0$, 4, 8, 12, 16, 20 μrad, and ∞. The integration was carried out by simple summation on a square grid with a spacing of 0.2 μrad along both axes. For better visibility, the curves for different values of T_θ have been shifted to achieve 0.2 spacing along the vertical axis. The lower curve corresponds to $T_\theta=0$ and the upper curve (for $T_\theta=\infty$ within the approximation considered) corresponds to pure two-wave diffraction.

As follows from the calculations, multiwave effects are displayed even with collimation of the beam to 20×20 μrad^2 in the form of a lower maximum of the principal reflection and additional regions of weak reflection. However, already with angular misorientation of the beam exceeding 10×10 μrad^2, the principal maximum is fully distinguishable and has a position on the energy scale corresponding to the two-wave case. This result can be utilized in calibrating monochromators with an energy resolution of the order of 1 meV.

4. TWO-WAVE DYNAMICAL DIFFRACTION, KINEMATIC DIFFRACTION, AND THE INFLUENCE OF OTHER REFLECTIONS ON THEIR PROPERTIES

Multiwave dynamical diffraction is described by the system of equations (6), which does not have an analytic solution in the general case. Moreover, the results of detailed studies only of cases of systematic diffraction, in which all the vectors of the reciprocal lattice lie in a single plane, have been published hitherto. In such cases the variation of the energy of the incident photons leads only to variation of the reference point on the plane of angular parameters without alteration of the angular dependence of the reflectivities. The case which we considered refers to nonsystematic (random)

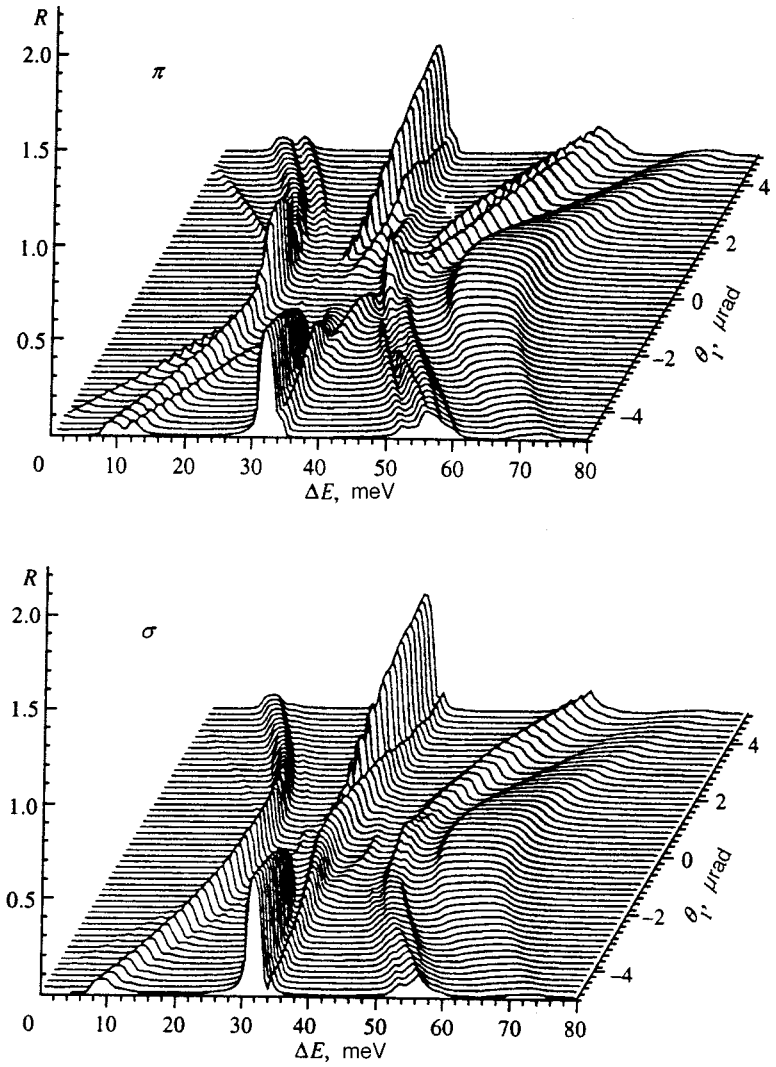

FIG. 3. Dependence of the reflectivity for (1,9,9) back reflection at $\theta_2=0$ for two polarization states of the incident wave.

diffraction in Chang's terminology.[17] Nevertheless, we can use the approximate approach previously developed for a qualitative analysis of the calculation results.

Let us consider the important special case where two of the set of parameters A_m characterizing the deviation from the Bragg conditions are close to one another, for example, the parameters with the indices i and j, while the remaining parameters have values differing strongly from these two. In this case it is natural to presume that only the components B_i and B_j of the eigenvector will have large and comparable values, while the remaining components will be small. We first consider the situation in which the small components can be completely neglected and the polarization can be separated. This corresponds to two-wave diffraction, for which in the system of equations (6) it is sufficient to retain only two equations:

$$(\varepsilon+A_i-H_{ii})B_i-H_{ij}B_j=0,$$

$$-H_{ji}B_i+(\varepsilon+A_j-H_{jj})B_j=0. \tag{15}$$

This system has two solutions, in which

$$\varepsilon_{1,2}=H_{ii}-A_i+0.5[-a\pm(a^2+4H_{ij}H_{ji})^{1/2}],$$

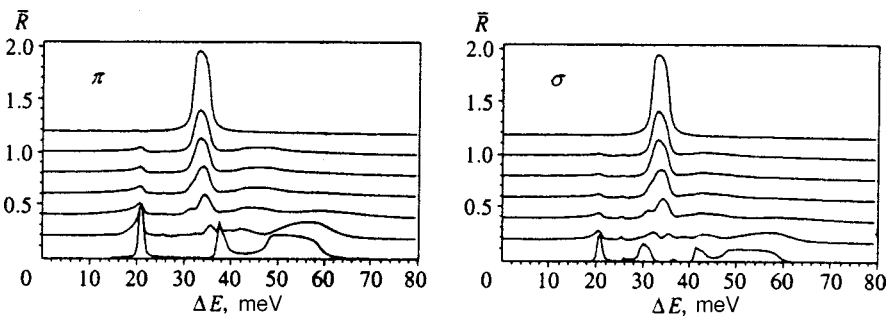

FIG. 4. Energy spectra of the angle-integrated back reflectivity for various values of the collimation of the incident beam: 0×0 (lower curve), 4×4, 8×8, 12×12, 16×16, $20\times20\,\mu\text{rad}^2$, and the two-wave case (upper curve). For better visibility the curves have been shifted along the vertical axis with 0.2 spacing.

$$a=(A_j-A_i)-(H_{jj}-H_{ii}),\ \ B_j/B_i=(\varepsilon+A_i-H_{ii})/H_{ij}. \tag{16}$$

Here the branch with a positive imaginary part is chosen for the square root.

If the index $i=0$ corresponds to the incident beam, and the index $j=h$ corresponds to the (1,9,9) back reflection, then in the approximation of a thick absorbing crystal, the reflection amplitude is exactly equal to the ratio between the components of the Bloch wave and can be written in the standard notation[1] as follows:

$$\frac{B_h}{B_0}=i\frac{p+\sqrt{p^2-4\beta\chi_h\chi_{\bar{h}}C}}{2\chi_{\bar{h}}}, \tag{17}$$

where

$$p=\alpha\beta-\chi_0(1+\beta),\quad \beta=\gamma_0/|\gamma_n|,\quad C=(\mathbf{e}_{0s}\mathbf{e}_{hs}). \tag{18}$$

Here it has been taken into account explicitly that $\gamma_h<0$. In the case of back reflection $\beta=1$. Equations (17) and (18) correspond exactly to the upper curve in Fig. 4 with consideration of the relation $\alpha=-4\theta_\omega=-4\Delta E/E_c$.

In the kinematic approximation, in which the rescattering between the weak components of the mixed Bloch wave for $m\neq i,j$ can be neglected and only the single scattering from strong waves into weak waves need be taken into account, the weak components are given by the following expression:

$$B_m=\frac{H_{mi}B_i+H_{mj}B_j}{\varepsilon+A_m-H_{mm}}. \tag{19}$$

As follows from this formula, ordinary single-wave single scattering from the incident wave with $i=(000)$ into the back reflection wave with $m=(1,9,9)$ can be enhanced in the presence of several strong waves, and the appearance of additional reflection maxima can be expected in the case where the Bragg condition is satisfied for some wave with $j\neq(1,9,9)$ and this wave is scattered in phase with the incident wave.

In addition, we can write the system of equations for strong waves in the more exact form

$$\begin{aligned}(\varepsilon+A_i-H_{ii})B_i-H_{ij}B_j&=\sum_m H_{im}B_m,\\ -H_{ji}B_i+(\varepsilon+A_j-H_{jj})B_j&=\sum_m H_{jm}B_m,\end{aligned} \tag{20}$$

where $m\neq i,j$ in the sum. Now, using formula (19 for weak waves and substituting it into (20), we obtain a system of the type (15), but with renormalized coefficients:

$$\begin{aligned}(\varepsilon+A_i-F_{ii})B_i-F_{ij}B_j&=0,\\ -F_{ji}B_i+(\varepsilon+A_j-F_{jj})B_j&=0,\end{aligned} \tag{21}$$

where

$$F_{kl}=H_{kl}+\sum_{m\neq i,j}\frac{H_{km}H_{ml}}{\varepsilon+A_m-H_{mm}},\quad k=i,j,\quad l=i,j. \tag{22}$$

Formulas like (19), (21), and (22) were obtained for a more general case with consideration of the polarization multipliers in Ref. 18 as a method for approximate solution of the problem. In Refs. 19–21 the mechanism for renormalization of the parameters was called virtual Bragg scattering. The same approach was used in Refs. 22 and 23 to investigate standing x-ray waves and total reflection in a forbidden reflection.

Under ordinary conditions for two-wave diffraction the parameter describing the deviation from the Bragg condition for a weak wave $A_m\gg\varepsilon$, H_{mm}, and the renormalization of the coefficient is very small. However, in a situation which is close to the pure multiwave situation, this renormalization is significant and can significantly distort the character of two-wave diffraction, i.e., can significantly shift the position of the maximum and alter its width and height. In this case even the magnitude of the dispersion correction should be calculated self-consistently.

Thus, an analysis of the multiwave corrections to the two-wave (1,9,9) back reflection reveals effects of two types. First, the two-wave back reflectivity peak is distorted as a result of the renormalization of the parameters of the scattering associated with rescattering on other reflections. Second, renormalization of the kinematic diffraction appears when the Bragg conditions for any of the other reflections are satisfied with consideration of the renormalization of its parameters. Significant interference of the two scattering channels then occurs, as a result of which, as the analysis showed, the single-band approximation does not provide the required accuracy in comparison to an exact multiwave calculation. Therefore, the formulas presented in this section are suitable only for a qualitative understanding of the results of the exact calculation presented in Figs. 2 and 3, but cannot be used directly for calculations.

The mechanism discussed here can also be considered in the case where the conditions for three-wave diffraction are satisfied simultaneously, as occurs at $\theta_1=0$. The formulas presented above can easily be generalized to this case. The situation is far more complicated when the regions of two-wave diffraction for different reflections are fairly close, but do not coincide exactly. In this case, the interference of different scattering channels leads to a complicated structure of peaks of kinematic scattering, as is clearly seen in Fig. 3.

We express our thanks to Yu. Shvyd'ko for formulating the problem and taking an interest in this work.

*)E-mail: kohn@kurm.polyn.kiae.su

[1] Z. G. Pinsker, *X-Ray Crystal Optics* [in Russian], Nauka, Moscow (1982).
[2] K. Kohra and T. Matsushita, Z. Naturforsch. A **27**, 484 (1972).
[3] O. Brümmer, H. R. Höche, and J. Nieber, Phys. Status Solidi A **53**, 565 (1979).
[4] A. Caticha and S. Caticha-Ellis, Phys. Rev. B **25**, 971 (1982).
[5] W. Graeff and G. Materlik, Nucl. Instrum. Methods Phys. Res. **195**, 97 (1982).
[6] V. I. Kushnir and É. V. Suvorov, JETP Lett. **44**, 262 (1986).
[7] R. Verbeni, F. Sette, M. H. Krisch, U. Bergmann, B. Gorges, C. Halcoussis, K. Martel, C. Masciovecchio, J. F. Ribois, G. Ruocco, and H. Sinn, J. Synchrotron Radiat. **3**, 62 (1996).
[8] A. Caticha, K. Aliberti, and S. Caticha-Ellis, Rev. Sci. Instrum. **67**, 1 (1996).

[9] Yu. V. Shvyd'ko, E. Gerdau, J. Jäschke, O. Leupold, M. Lucht, and H. Ruter, Phys. Rev. B **57**, 4968 (1998).
[10] Yu. V. Shvyd'ko *et al.*, submitted to Hyperfine Interactions (1999).
[11] A. I. Chumakov, R. Rüffer, A. O. R. Baron, H. Grünsteudel, H. F. Grünsteudel, and V. G. Kohn, Phys. Rev. B **56**, 10 758 (1997).
[12] V. G. Kohn, A. I. Chumakov, and R. Rüffer, Phys. Rev. B **58**, 8437 (1998).
[13] V. G. Kohn, Phys. Status Solidi A **54**, 375 (1979).
[14] V. G. Kohn, J. Mosc. Phys. Soc. **1**, 425 (1991).
[15] V. G. Kohn, Zh. Éksp. Teor. Fiz. **105**, 665 (1994) [JETP **78**, 357 (1994)].
[16] S. A. Stepanov, http://sergey.bio.aps.anl.gov.
[17] S. L. Chang, *Multiple Diffraction of X Rays in Crystals*, Springer-Verlag, Berlin (1984) [Russ. transl., Mir, Moscow (1987)].
[18] R. Hoier and K. Martinsen, Acta Crystallogr. A **25**, 854 (1983).
[19] L. D. Chapmann, D. R. Yoder, and R. Colella, Phys. Rev. Lett. **46**, 1578 (1981).
[20] R. Colella, Z. Naturforsch. A **37**, 437 (1982).
[21] M. C. Schmidt and R. Colella, Phys. Rev. Lett. **55**, 715 (1985).
[22] V. G. Kon, Kristallografiya **33**, 567 (1988) [Sov. Phys. Crystallogr. **33**, 333 (1988)].
[23] V. G. Kohn, Phys. Status Solidi A **106**, 31 (1988).

Translated by P. Shelnitz